Reduced impact logging minimally alters tropical rainforest carbon and energy exchange

Scott D. Miller[a,1], Michael L. Goulden[b], Lucy R. Hutyra[c], Michael Keller[d], Scott R. Saleska[e], Steven C. Wofsy[f], Adelaine Michela Silva Figueira[g], Humberto R. da Rocha[h], and Plinio B. de Camargo[i]

[a]Atmospheric Sciences Research Center, State University of New York, Albany, NY 12203; [b]Department of Earth System Science, University of California, Irvine, CA 92697; [c]Department of Geography and Environment, Boston University, Boston, MA, 02215; [d]International Institute of Tropical Forestry, US Department of Agriculture Forest Service, San Juan, Puerto Rico 00928; [e]Department of Ecology and Evolutionary Biology, University of Arizona, Tuscon, AZ 85721; [f]Department of Earth and Planetary Sciences, Harvard University, Cambridge, MA 02138; [g]Department of Biology, Federal University of Western Pará, Pará, Brazil 68040-070; [h]Department of Atmospheric Sciences, University of Sao Paulo, Sao Paulo, Brazil 05508-090; and [i]Centro de Energia Nuclear na Agricultura, University of Sao Paulo, Sao Paulo, Brazil 13416-000

Edited* by Stephen W. Pacala, Princeton University, Princeton, NJ, and approved October 24, 2011 (received for review March 30, 2011)

We used eddy covariance and ecological measurements to investigate the effects of reduced impact logging (RIL) on an old-growth Amazonian forest. Logging caused small decreases in gross primary production, leaf production, and latent heat flux, which were roughly proportional to canopy loss, and increases in heterotrophic respiration, tree mortality, and wood production. The net effect of RIL was transient, and treatment effects were barely discernable after only 1 y. RIL appears to provide a strategy for managing tropical forest that minimizes the potential risks to climate associated with large changes in carbon and water exchange.

Brazil | Amazon | land use | micrometeorology

Deforestation in the tropics affects the land–atmosphere exchange of trace gases and energy in ways that may impact regional and global climate. Tropical deforestation contributed 16% (1.5 PgC y^{-1}) of human-induced CO_2 emissions during 2000–2006 (1), while increasing land-surface albedo and decreasing available energy and evapotranspiration (2). The changes in surface–energy exchange and increase in atmospheric CO_2 associated with large-scale tropical deforestation are predicted to alter precipitation patterns (3, 4) and cause a net warming of global climate (5, 6). The avoidance of tropical deforestation as a means to slow the rise of atmospheric carbon dioxide, while maintaining the role of forest in the water and energy cycles and sustaining biodiversity and other environmental services, is a key climate change mitigation goal (e.g., the United Nations program Reducing Emissions from Deforestation and Forest Degradation) (7, 8).

The harvesting of marketable trees by selective logging in the Brazilian Amazon has occurred at an areal rate comparable to deforestation ($1–2 \times 10^4$ km^2 y^{-1} between 1996 and 2002) (9–11). Conventional logging (CL) is highly damaging to forest canopy, residual vegetation, and soil (12), and increases forest susceptibility to fire (11). The estimated gross CO_2 emission to the atmosphere from CL in the Amazon amounts to 25% of that due to deforestation (9). In contrast, reduced impact logging (RIL) is intended to minimize the disruption of tropical forest carbon and water cycles (13) via preharvest tree selection and vine cutting, directional felling, and planned extraction (skid) trails and log decks. RIL has been shown to reduce canopy destruction (12, 14–16); however, the effects of RIL on land-atmosphere gas and energy exchange have not been well quantified.

We report direct measurements of the net effect of RIL on tropical forest carbon, water, and energy exchange. Two sites in the Tapajos National Forest (TNF) were studied as part of the Large-Scale Biosphere-Atmosphere Experiment in Amazonia (17), denoted by distance south of Santarem, Para, Brazil (Fig. S1): "km 67" (unlogged control site, 2.85667 S, 54.958889 W) and "km 83" (logged site, 3.01803 S, 54.97144 W). The logging was conducted by a local commercial firm (Empresa Agropecuária Treviso Ltda), with oversight from the Brazilian Institute for the Environment and Renewable Resources. Parallel measurements at control and logged sites began 6–12 mo before logging, and continued at least 29 mo afterward. Our measurements focused on aspects of tropical forest–atmosphere exchange that under large-scale land-use change are expected to affect climate: carbon and energy fluxes, net carbon storage, soil moisture, and albedo.

Results

Loggers cut 3.6 trees ha^{-1}, which created 2.5 canopy gaps ha^{-1} and decreased canopy coverage from 96% to 88% (18). The extent of canopy destruction because of RIL was far less than the 30% loss reported for CL (12). The logged trees accounted for 7–10% of the forest's initial above-ground live biomass (AGLB; 168 MgC ha^{-1}) (Table S1). The amount of bole wood removed (5.0–6.8 MgC ha^{-1}) was slightly less than the average for the overall Amazon basin [7.3 MgC ha^{-1} (11)]. Fifteen additional trees were killed or damaged for each tree logged at km 83 (19). Logging generated 13.2–18.2 MgC ha^{-1} of coarse woody debris, 95% left on the forest floor, and 5% as standing dead trees. The total carbon either removed or killed was thus 18–25 MgC ha^{-1}, or 11–15% of initial AGLB.

Logging had a marked effect on the patterns of production. We partitioned aboveground wood production into three size classes: small subcanopy trees with diameter at breast height (DBH; 1.3 m) 10–35 cm, medium midcanopy trees with DBH 35–55 cm, and large upper-canopy trees with DBH 55–100 cm (20). Wood production before logging exhibited a strong maximum corresponding to tree heights at the mid-to-upper canopy levels (~25 m) (Fig. 1*A*, open squares). Wood production in the lower canopy more than doubled following logging (Fig. 1*A*, solid circles and hatched area), and the mean tree height of production descended from 26 to 24 m. Stimulation of tree growth, especially near gaps, was likely caused by increased light penetration and facilitated by the low levels of damage to the canopy and subcanopy (21).

The changing patterns of production among tree-size classes (Fig. 1*A*) did not translate into large shifts in whole-stand carbon fluxes, as measured by eddy covariance. The time series of gross photosynthesis [gross ecosystem exchange (GEE); positive flux indicates uptake by the forest] (Fig. 2*A*) and respiration (R; positive flux indicates loss from the forest) (Fig. 2*B*) showed no distinct changes following logging (Fig. 2 *A* and *B*). Differences in GEE and R between logged and control sites were smaller

Author contributions: M.L.G., S.R.S., S.C.W., H.R.d.R., and P.B.d.C. designed research; S.D.M., M.L.G., L.R.H., S.R.S., A.M.S.F., and H.R.d.R. performed research; S.D.M., L.R.H., S.R.S., A.M.S.F., and H.R.d.R. analyzed data; and S.D.M., M.L.G., M.K., and S.C.W. wrote the paper.

The authors declare no conflict of interest.

*This Direct Submission article had a prearranged editor.

[1]To whom correspondence should be addressed. E-mail: smiller@albany.edu.

This article contains supporting information online at www.pnas.org/lookup/suppl/doi:10.1073/pnas.1105068108/-/DCSupplemental.

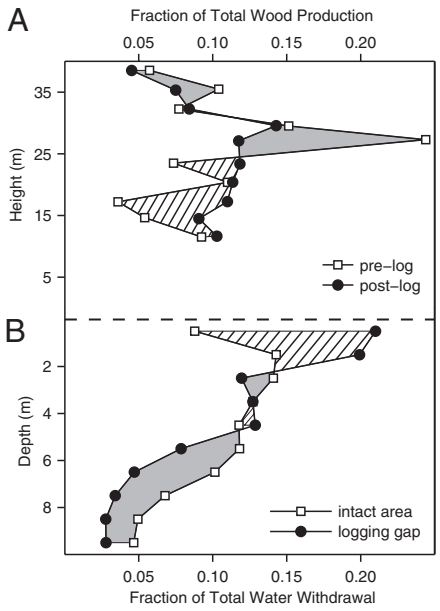

Fig. 1. Ground-based measurements of carbon accumulation in wood and soil water withdrawal at the logged site in Tapajos National Forest, Para, Brazil. (*A*) Wood production versus tree height before (November 2000–September 2001, open squares) and after (October 2001–March 2004, solid circles) logging for 734 trees, normalized by total wood production. (*B*) Water withdrawal versus depth at the logged site measured during the 2002 dry season (August–November) in an intact area (open squares) and within a logging gap (filled circles), normalized by total column water withdrawal for the same period. In both panels, the hatched (shaded) region corresponds to increased (decreased) activity after logging.

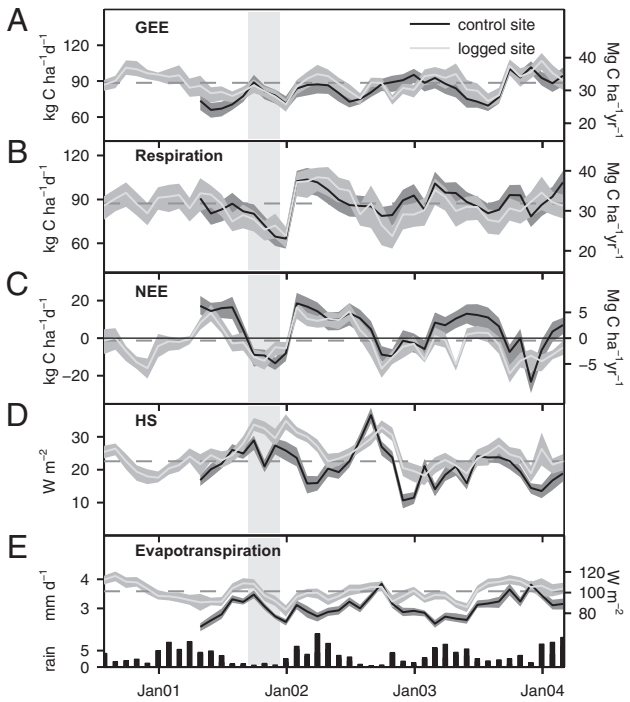

Fig. 2. Monthly forest-atmosphere fluxes of carbon ($kgC{\cdot}ha^{-1}{\cdot}d^{-1}$ and $MgC{\cdot}ha^{-1}{\cdot}y^{-1}$) and energy ($W{\cdot}m^{-2}$) at the control (km 67, dark curve) and logged (km 83, light curve) sites in Tapajos National Forest, Para, Brazil: (*A*) GEE (positive to forest); (*B*) respiration (positive to atmosphere); (*C*) NEE (positive to atmosphere); (*D*) sensible heat flux; and (*E*) evapotranspiration and precipitation ($mm\ d^{-1}$). Shaded areas about curves correspond to 95% percent confidence intervals because of sampling error, gap filling, and (*A–C*) the u_*-filter cutoff (0.17–0.27 $m\ s^{-1}$). Vertical shaded region September 15 to December 15 2001 indicates logging period. Horizontal dashed lines indicate the logged-site average during period before logging.

than the uncertainty in the monthly averaged time series (overlapping shaded regions in Fig. 2 *A* and *B*). The small effect of RIL on the carbon fluxes is emphasized by the similarity of net ecosystem exchange (NEE; R – GEE), both magnitude and seasonal variation, between logged and control sites (Fig. 2*C*).

Similarly, the cumulative rates of net and gross CO_2 exchange did not change markedly following logging. We summed the fluxes for 6- and 12-mo periods, and calculated the differences between sites (Δ = the difference between km 83 and km 67) to obtain ΔGPP (gross primary production), ΔR, and ΔNEE before and after logging (Table S2). GPP at km 83 decreased relative to km 67 ($\Delta GPP_{postlog} - \Delta GPP_{prelog}$ was negative) by 2–3 $MgC{\cdot}ha^{-1}{\cdot}y^{-1}$ following logging (Fig. 3*A*), which corresponds to a ∼10% decline that is comparable to the observed decrease in the area of intact forest canopy. R at km 83 increased slightly in the first year following logging ($\Delta R_{postlog} - \Delta R_{prelog}$ was positive), and subsequently declined in years 2 and 3 (Fig. 3*B*). $\Delta NEE_{postlog} - \Delta NEE_{prelog}$ was 2–3 $MgC{\cdot}ha^{-1}{\cdot}yr^{-1}$ during the first year after logging (Fig. 3*C*), corresponding to a net release of carbon to the atmosphere. ΔNEE was indistinguishable from the prelogging period in years 2 and 3 (Fig. 3*C*).

Ecosystem carbon budgets were constructed before and after logging (Fig. 4 and Table S3). Total respiration was partitioned into autotrophic (R_a) and heterotrophic (R_h) sources by combining the micrometeorological and ecological measurements (see *Materials and Methods*). Autotrophic respiration decreased by 9% (3 $MgC{\cdot}ha^{-1}{\cdot}y^{-1}$), which was similar to the declines in GPP, intact canopy area, and AGLB. About half the R_a decrease was offset by increasing decomposition (R_h), resulting in a 1.5 $MgC{\cdot}ha^{-1}{\cdot}y^{-1}$ decrease in total R (Fig. 3*B*). Similarly, much of the increase in wood production at the logged site was offset by a 10% decrease in leaf production (leaf net primary production, NPP_{leaf}), resulting in a small increase in total NPP (assuming constant NPP_{root}).

The logging had a marked effect on the local patterns of soil water content and withdrawal. Soil water dynamics following logging were measured in two 10-m profiles at km 83, one in intact forest and the other in a logging gap (22). A larger proportion of water was extracted from shallower depths in the logging gap, and the mean depth of withdrawal shifted from 4 m in the intact forest to 3 m in the logging gap (Fig. 1*B*, hatched area versus shaded area). A portion of the 40% decrease in water withdrawal in the gap relative to the intact area was likely because of the loss of canopy and hypothesized decrease in live root density. The mature trees that were harvested may have been deeply rooted compared with the small stems that grew up in the gap.

Logging had modest and transient effects on the water and energy fluxes by the entire ecosystem. Changes in water and heat flux were smaller than the interseasonal and interannual variability (Fig. 2 *D* and *E*, and Table S2). Sensible heat flux at the logged site increased by several watts per square meter relative to the control site, corresponding to a change of about 10% (Fig. 3*D*). Latent heat flux decreased by a slightly larger amount (3–4 $W{\cdot}m^{-2}$) (Fig. 3*E*). The ratio of sensible to latent heat flux (the Bowen ratio) increased from 0.2 to 0.3 at the logged site in the first year after logging, but returned to the prelogging ratio by year 3. Logging had no discernable effect on the km 83 albedo determined by the National Aeronautics and Space Administration's MODIS (Moderate Resolution Imaging Spectroradiometer) sensors (Table S4). The proportional changes in the heat fluxes and canopy loss, and the lack of change in albedo, imply the shifts in

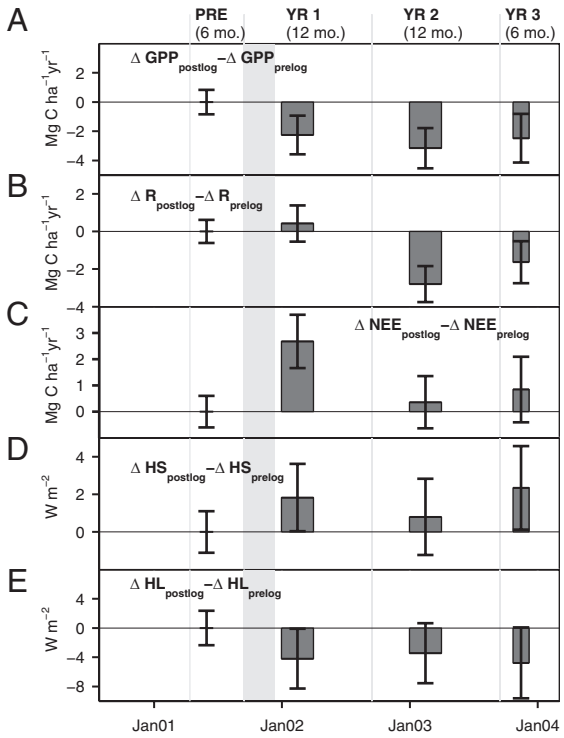

Fig. 3. Differences in forest-atmosphere carbon (MgC·ha^{-1}·y^{-1}) and energy (W·m^{-2}) fluxes, calculated as (Δ = logged − unlogged), in Tapajos National Forest, Para, Brazil. The flux difference for the period before logging was subtracted from each postlogging period. (*A*) GPP (positive to forest); (*B*) respiration (positive to atmosphere); (*C*) NEE (positive to atmosphere); (*D*) sensible heat flux; and (*E*) latent heat flux. Vertical shaded region September 15 to December 15, 2001 indicates logging period. Error bars correspond to 95% percent confidence intervals because of sampling error and gap filling.

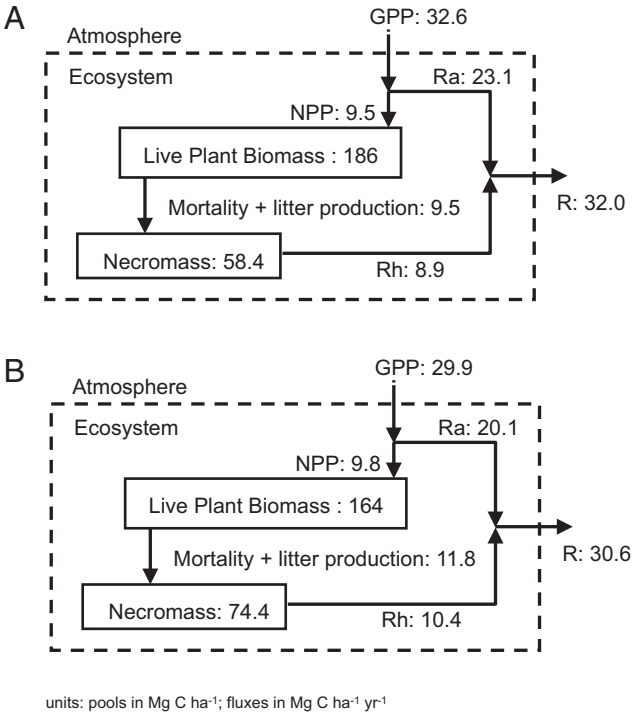

Fig. 4. Carbon pools (boxes, MgC ha^{-1}) and fluxes (arrows, MgC·ha^{-1}·y^{-1}): (*A*) before logging; and (*B*) for the 3-y period following logging (Table S3). Carbon pools include live plant biomass (186 MgC ha^{-1}) (34), necromass (58.4 MgC ha^{-1}) (53), and soil mineral carbon (71 MgC ha^{-1}) (54).

sensible and latent heat flux were driven by the loss of canopy and not a change in available energy.

Discussion

Logging resulted in a small, transient net source of CO_2 to the atmosphere, mostly in the first year, presumably because of the rapid decomposition of fine logging debris (23, 24). The first-year carbon emission at the logged site was 2.4–2.7 MgC ha^{-1}, which is less than 10% of GPP and less than 2% of the original aboveground biomass. RIL-induced greenhouse gas forcing caused by soil emissions of N_2O, CH_4, and CO_2 were small (25). Off-site carbon emissions caused by decomposition or combustion of short-lived products and mill waste were estimated to be 3 MgC ha^{-1}, assuming one-third of the bole wood removed from the site ended up as long-lived products (26). The total equivalent carbon emission was ~6 MgC ha^{-1}, less than 4% of the forest's 168 MgC ha^{-1} AGLB, and much smaller than the 150 MgC ha^{-1} (90% of AGLB) that would have been released by deforestation (27). Because half of the net CO_2 emission was estimated to occur from the processing of harvested boles, improvements in milling and conversion of biomass to energy could further mitigate carbon emissions.

The changes in several key ecosystem processes [GPP, NPP_{leaf}, latent heat flux (HL)] were in direct proportion to canopy loss, which underscored the importance of minimizing canopy destruction. The ability of the forest to maintain NPP despite the loss of canopy, and the increased allocation of carbon to stem production, point to a rapid restoration of biomass following disturbance. Fig. 2 suggests carbon uptake at the logged site accelerated relative to the control site throughout the postlogging period. Interestingly, the NPP:GPP ratio, a measure of carbon use efficiency, increased from 0.29 to 0.35 after RIL treatment.

Albedo was unaffected by RIL, whereas nearby deforestation increased albedo by 0.01–0.03 (Table S4). The shifts in sensible and latent heat flux following RIL were smaller than the 20–40% changes reported for conversion to pasture in the southwestern Amazon (2), and, importantly, the changes following RIL persisted for just 1 or 2 y, whereas changes associated with deforestation were sustained. Similarly, although measurements of canopy gap microclimate following RIL showed warmer and drier conditions near the ground compared with undisturbed forest (18), the rapid reestablishment of the hydrological cycle suggests that any increased fire risk was small and transient, as fire susceptibility at TNF is determined primarily by relative humidity at the forest floor rather than fuel loading (28).

Simulations of RIL at TNF showed potential for long-term sustainability with a 30-y cut cycle (29). In contrast, other model studies for lowland Amazonian forests have predicted substantial decreases in harvest volume with a similar cut cycle, even at low RIL intensities (7, 30). At high intensities, models have predicted degradation of forest biodiversity and ecosystem functioning (15). These studies conclude that longer cut cycles and postlogging silvicultural interventions are necessary to maintain sustainable timber yields (31, 32). Our measurements captured only the immediate effects of RIL on carbon and energy fluxes; the effects on tree mortality, demographic shifts, and changes in wood production beyond the 3-y study interval are uncertain.

RIL for the 3,130-ha tract logged at TNF was highly profitable (33). Overall revenue from wood was $830.00 US ha^{-1}, compared with costs of $610.00 US ha^{-1}; thus, RIL resulted in an internal rate of return (IRR) of 36%, much higher than the most profitable cattle projects studied in the Amazon (IRR up to 12%) (33). The km 83 logging generated high-paying jobs by local standards at a rate of one person used for every 14-ha

logged, with 60% of positions filled by residents of local communities by the end of the project.

Cumulative deforestation in the Brazilian Amazon reached 18% of the original forested area in 2008 (10). At an average rate of 1.7×10^4 km^2 y^{-1} (2001–2008) (10), business-as-usual scenarios imply that as much as 35% of Amazon rain forests could be cleared by 2040, contributing up to 4% of anthropogenic carbon emissions, altering the energy balance, and warming the climate. In contrast, with net carbon emission just 4% of that typical of deforestation, RIL has the potential to significantly reduce the impact of tropical land use on land–atmosphere exchange.

Materials and Methods

The logged site was within a 700-ha area that was part of a larger, 3,130-ha RIL demonstration project over a 5-y period beginning in 1999. The logging at the km 83 flux tower site occurred between August and December 2001, resulting in a logged area that extended 1 to 3 km east and north of the flux tower.

Canopy Gaps. After the logging, gap location, size, and shape were mapped in a 600-m × 300-m area that extended 500 m to the northeast of the logged-site flux tower. The logging created 44 new gaps, which ranged in size from single tree falls, which were ~10-m across, to log landings used to temporarily store boles, which were ~50-m across (18).

Ecological Measurements. Initial surveys of tree DBH were used along with allometric equations developed for moist tropical forests (34) to calculate above-ground live biomass in 1999, 2001, and 2005 at the control site (35), and 2000 at the logged site (36). Large (55–100 cm) and medium (35–55 cm) trees were measured in a 20-ha plot at the control site, and a 48-ha area at the logged site; small (10–35 cm) trees were measured in a 4-ha subsample at the control site, and a 1.8-ha subsample at the logged site. The survey datasets are available online (37, 38).

Wood production was measured using dendrometer bands to monitor changes in tree DBH (39). At the control site, 763 bands were installed on 529 small, 119 medium, and 115 large trees in a 20-ha area east of the flux tower in 1999 (35). At the logged site, 691 bands were installed on 363 small, 223 medium, and 105 large trees in an 18-ha area east of the tower between November 2000 and February 2001. DBH increments were measured every 4 wk at the control site and every 6 wk at the logged site. The cumulative DBH increment for each tree at the control site was calibrated so that the long-term increment matched the measured change in DBH between the 2001 and 2005 surveys. Tree mass and height were calculated for each DBH measurement (20, 40), and wood production between measurement intervals was calculated from changes in tree mass. For each tree-size class, wood production was calculated as the product of the mean per tree growth rate and the stem density for that size class (Table S5). Uncertainties in wood production rates reflect the variability (95% confidence interval) in growth rates within a tree-size class. The wood production datasets are available online (41, 42).

Litterfall (NPP_{leaf}), including leaves, fruit, and wood were collected in litter baskets east of each flux tower at 2-wk intervals, and were used to calculate fine litter production. The litterfall data are available online (41, 43).

Micrometeorological Measurements. Carbon and energy flux at each site were measured from a 67-m tall, 46-cm triangular cross-section tower (Rohn 55G, Peoria IL). The logged site tower operated for 1,353 d (32,496 h) between July 1, 2000 and March 13, 2004 (44). The control site tower operated for 1,733 d (41,592 h) between April 13, 2001 and January 9, 2006 (45). Measurements at both sites were terminated by tree falls that destroyed the towers. The CO_2 profile between the surface and the height of the eddy covariance instrumentation was measured and used to calculate changes in CO_2 storage within the air column below the flux sensors (F_s). Turbulent CO_2 flux (F_c) and storage were combined to estimate NEE for each flux interval as $NEE = F_c + F_s$. Data retention rates for carbon and water fluxes were 75–88% at both sites. Methodology used to measure and calculate fluxes, fill data gaps, and to correct for flux loss during conditions with poor vertical mixing (u_*-filter) have been published (36, 45, 46), and the flux data sets are available online (47–49).

Missing meteorological variables and turbulent fluxes were gap-filled using mean diurnal variation with a 40-d window (46). Missing NEE was filled using a light-response model (50). Uncertainties in NEE because of sampling uncertainty and gap filling of missing data were estimated using a bootstrap method (46). The uncertainty in the carbon fluxes (NEE, GPP, R) because of the u_*-filter was estimated by calculating the carbon fluxes using a range of u_*-filter cutoffs from 0.17 m s^{-1} to 0.27 m s^{-1} to generate time series of NEE, GPP, and R representing lower and upper bounds of plausible carbon exchange (e.g., $NEE_{0.17}$ and $NEE_{0.27}$). The uncertainty in the carbon exchange because of the choice of the u_*-filter cutoff was calculated as the larger of the differences $NEE_{0.22} - NEE_{0.17}$ (lower bounds) and $NEE_{0.27} - NEE_{0.22}$ (upper bounds), and was added to the sampling and gap filling uncertainty estimates to calculate the total uncertainty at each site (Fig. 2 *A–C*, and Table S2). It was previously shown that a u_*-filter cutoff of 0.22 m s^{-1} (e.g., $NEE_{0.22}$) provided the best estimate of ecosystem respiration at both sites (46); therefore, the u_*-filtering uncertainty was not included in the differences in carbon fluxes between the sites (ΔGPP, ΔR, ΔNEE) in Fig. 3 *A–C*, and Table S2.

Soil Moisture Measurements. Soil moisture measurements were made at the logged site from March 2002 to December 2003 in two 10-m deep soil pits (1 × 2 m^2 area) within 50 m of the micrometeorological tower (22). Both pits were within the selectively logged area: one within an intact area of forest, the other within a gap created by the logging. Soil water content was measured at 0.1 Hz using water content reflectometers (CS615-G, Campbell Scientific) installed horizontally into the walls of the pits at 0.15, 0.3, 0.6, 1, 2, 3, 4, 6, 8, and 10 m. Soil water withdrawal was calculated as the difference between the profile measured at the beginning (first 2 wk of August 2002) and end (last two weeks of October 2002) of the dry season. The soil moisture datasets are available online (51).

Albedo. Satellite 8-d composite time series of 500-m MODIS albedo for the km 83 and km 67 sites, and also for a nearby pasture (km 77), were obtained from the Distributed Active Archive Centers Land Products Web site (http://daac.ornl.gov/MODIS/). The data included 1 y before logging and 3 y after logging at each site (Table S4). Shortwave albedo data were used with default solar zenith angle (local solar noon) and optical depth (0.2). At the forest sites, mean albedo for each 8-d composite was calculated for an 18.8-ha area east of the flux tower, 3.5 km (7 pixels) in east-west direction and 2.5 km (5 pixels) in the north-south direction. At the pasture site, a 0.5-km^2 area (2 pixels east-west, 1 pixel north-south) was used. The uncertainty in albedo was estimated by bootstrapping.

Ecosystem Carbon Budget. An ecosystem carbon budget at the logged site was constructed for the year before logging and the 3-y period after logging by combining the micrometeorological and ecological measurements. The relationships between the carbon pools and fluxes are sketched in Fig. 4 and tabulated in Table S3.

For micrometeorological fluxes (GPP, R, NEE), the prelogging flux ($X_{prelog,\ 12\ mos.}$) was calculated as the average for the 12-mo period before logging. The difference between the post- and prelogging flux at the logged site, δX_{total}, was assumed to include contributions due to the logging, $\delta X_{logging}$, and caused by interannual differences in climate or "weather," $\delta X_{weather}$, such that $\delta X_{total} = X_{postlog} - X_{prelog} = \delta X_{logging} + \delta X_{weather}$, where, for simplicity, measurement error is not denoted; however, its calculation is detailed below. The weather-induced contribution was assumed to be equal at the two sites, $\delta X_{weather} = \delta X_{weather,\ km\ 67}$, and the difference in post- and prelogging flux at km 67 (the unlogged site) was assumed entirely because of weather, $\delta X_{total,km67} = \delta X_{weather,km67} = X_{postlog,km67} - X_{prelog,km67}$. Rearranging these expressions gives $\delta X_{logging} = (X_{postlog} - X_{postlog,km67}) - (X_{prelog} - X_{prelog,km67}) = \Delta X_{postlog} - \Delta X_{prelog}$, where the Δ notation was used in the main text and plotted in Fig. 3. This expression was evaluated using only periods with in situ data at both sites. The postlogging flux was calculated as the sum $X_{postlog} = X_{prelog,12mo} + \delta X_{logging}$. The uncertainty in the ΔX terms was calculated as the square root of the sum of the squared uncertainties of X at the logged and unlogged sites (i.e., their errors were assumed uncorrelated). Similarly, the uncertainty in δX was calculated as the square root of the sum of the squared uncertainties of ΔX_{prelog} and $\Delta X_{postlog}$ (i.e., errors before and after logging were assumed uncorrelated).

NPP was calculated as the sum of wood, leaf, and root production, $NPP = NPP_{wood} + NPP_{leaf} + NPP_{root}$, where wood production and leaf production at each site were measured by dendrometers and litter baskets Table S3 and NPP_{root} was assumed constant and equal to 2.5 ± 0.5 MgC·ha^{-1}·y^{-1} (21), where 20% uncertainty in root production was assumed (52). Litter production (above and below ground) was calculated as the sum of NPP_{leaf} and NPP_{root}, assuming belowground root litter was in steady state with root production. The uncertainty in NPP and in litter production was calculated as the square root of the sum of squared uncertainties of the component fluxes (i.e., uncertainties were assumed uncorrelated).

Mortality at the logged site before logging (1.7 MgC·ha^{-1}·y^{-1}) was assumed in steady state with wood production (36), and after logging was 4.5 MgC·ha^{-1}·y^{-1} (21). Mortality at the control site was 2.4 MgC·ha^{-1}·y^{-1} (35).

The uncertainty in mortality at the logged site was assumed to be 30% (35). The change in live biomass was calculated as NPP minus the sum of mortality and litter production, and the change in necromass calculated as net ecosystem production (NEP) minus the change in live biomass (Fig. 4). The uncertainties in changes in live and dead biomass were calculated as the square root of the sum of squares of the component fluxes.

Autotrophic respiration (Ra) was calculated as GPP − NPP, and decomposition (heterotrophic respiration, Rh) was calculated as Rh = R − Ra (Fig. 4). The uncertainties in Rh and Ra were calculated as the square root of the sum of squares of the component fluxes.

Additional uncertainty was included in the carbon budget (Table S3) to account for the fact that overlapping data at the control and logged sites before logging covers only part of a year (seasonality effect). The carbon budget was recalculated using only data collected between March and September in each year after logging, to match with the months of data overlap in the prelogging period. For each carbon flux in the budget, the magnitude of the difference between the budget calculated using all months and using only March to September was used as an estimate of this additional uncertainty, and was added to the statistical sources of uncertainty described above.

ACKNOWLEDGMENTS. We thank Mary Menton, Antonio Oviedo, Helber Freitas, Marcy Litvak, Edward Lloyd Read, Robert Elliot, Chris Doughty, Dan Hodkinson, Lisa Zweede, Bethany Reed, and Johan Zweede for logistical and field support; the Brazilian Institute for the Environment and Renewable Resources, National Aeronautics and Space Administration, and Instituto Nacional de Pesquisas Espaciais for agency support; Conselho Nacional de Pesquisas for student stipends; the Brazilian Ministry of Science and Technology for their leadership of the Large-Scale Biosphere–Atmosphere Experiment in Amazonia; and Brazil's National Institute for Amazon Research for their management of that program. This work was supported by the US National Aeronautics and Space Administration Awards to the University of California at Irvine (Goddard NCC5-280), Harvard University (NNG06GG69A), and the State University of New York at Albany (NNG06GD29A).

1. Canadell JG, et al. (2007) Contributions to accelerating atmospheric CO2 growth from economic activity, carbon intensity, and efficiency of natural sinks. *Proc Natl Acad Sci USA* 104:18866–18870.
2. Von Randow C, et al. (2004) Comparative measurements and seasonal variations in energy and carbon exchange over forest and pasture in South West Amazonia. *Theor Appl Climatol* 78(1):5–26.
3. Dickinson RE, et al. (1989) Implications of tropical deforestation for climate: A comparison of model and observational descriptions of surface energy and hydrological balance. *Philos Trans R Soc Lond B Biol Sci* 324:423–431.
4. Werth D, Avissar R (2002) The local and global effects of Amazon deforestation. *J Geophys Res*, 107:8087, 10.1029/2001JD000717.
5. Salati E, Nobre CA (1991) Possible climatic impacts of tropical deforestation. *Clim Change* 19(1):177–196.
6. Bala G, et al. (2007) Combined climate and carbon-cycle effects of large-scale deforestation. *Proc Natl Acad Sci USA* 104:6550–6555.
7. Sist P, Ferreira FN (2007) Sustainability of reduced-impact logging in the Eastern Amazon. *For Ecol Manage* 243:199–209.
8. Miles L, Kapos V (2008) Reducing greenhouse gas emissions from deforestation and forest degradation: Global land-use implications. *Science* 320:1454–1455.
9. Asner GP, et al. (2005) Selective logging in the Brazilian Amazon. *Science* 310: 480–482.
10. INPE (2010) Monitoring of the Brazilian Amazon forest by satellite: 1988–2009. Available at: www.obt.inpe.br/prodes/prodes_1988_2009.htm. Accessed November 5, 2011.
11. Nepstad DC, et al. (1999) Large-scale impoverishment of Amazonian forests by logging and fire. *Nature* 398:505–508.
12. Pereira R, Zweede J, Asner GP, Keller M (2002) Forest canopy damage and recovery in reduced-impact and conventional selective logging in eastern Para, Brazil. *For Ecol Manage* 168(1-3):77–89.
13. Uhl C, et al. (1997) Natural resource management in the Brazilian Amazon. *Bioscience* 47(3):160–168.
14. Johns JS, Barreto P, Uhl C (1996) Logging damage during planned and unplanned logging operations in the eastern Amazon. *For Ecol Manage* 89(1-3), pp59–77.
15. Pinard MA, Putz FE (1996) Retaining forest biomass by reducing logging damage. *Biotropica* 28:278–295.
16. Veríssimo A, Barreto P, Mattos M, Tarifa R, Uhl C (1992) Logging impacts and prospects for sustainable forest management in an old Amazonian frontier: The case of Paragominas. *For Ecol Manage* 55(1-4):169–199.
17. Keller M, et al. (2004) Ecological research in the Large-scale Biosphere-Atmosphere Experiment in Amazonia: Early results. *Ecol Appl* 14(4):S3–S16.
18. Miller SD, Goulden ML, da Rocha HR (2007) The effect of canopy gaps on subcanopy ventilation and scalar fluxes in a tropical forest. *Agric For Meteorol* 142(1):25–34.
19. de Sousa CAD, Elliot JR, Read EL, Figueira AM (2011) LBA-ECO CD-04 Logging Damage, km 83 Tower Site, Tapajos National Forest, Brazil. *Oak Ridge National Laboratory Distributed Active Archive Center*Available at: http://daac.ornl.gov.
20. Nogueira EM, Nelson BW, Fearnside PM, França MB, Oliveira Á (2008) Tree height in Brazil's "arc of deforestation": Shorter trees in south and southwest Amazonia imply lower biomass. *Forest Ecol Manag* 225:2963–2972.
21. Figueira AMS, et al. (2008) Effects of selective logging on tropical forest tree growth. *J Geophys Res* 113:G00B05.
22. Bruno RD, da Rocha HR, de Freitas HC, Goulden ML, Miller SD (2006) Soil moisture dynamics in an eastern Amazonian tropical forest. *Hydrol Process* 20:2477–2489.
23. Bormann FH, Likens GE (1979) *Pattern and Process in a Forested Ecosystem* (Springer-Verlag, New York).
24. Sprugel DG (1985) Natural disturbance and ecosystem energetics. *The Ecology of Natural Disturbance and Patch Dynamics*, eds Pickett S, White P (Academic, New York), pp 335–352.
25. Keller M, et al. (2005) Soil–atmosphere exchange of nitrous oxide, nitric oxide, methane, and carbon dioxide in logged and undisturbed forest in the Tapajós National Forest, Brazil. *Earth Interact* 9(23):1–28.
26. Jenkins MB, Smith ET (1999) *The Business of Sustainable Forestry: Strategies for an Industry in Transition* (Island Press, Washington, DC).
27. Houghton RA, et al. (2000) Annual fluxes of carbon from deforestation and regrowth in the Brazilian Amazon. *Nature* 403:301–304.
28. Ray D, Nepstad D, Moutinho P (2005) Micrometeorological and canopy controls of fire susceptibility in a forested Amazon landscape. *Ecol Appl* 15:1664–1678.
29. Keller M, Asner GP, Silva JMN, Palace M (2004) *Working Forests in the Neotropics: Conservation through Sustainable Management?* eds Zarin DJ, Alavalapati J, Putz FE, Schmink M (Columbia University Press, New York), pp 41–63.
30. Dauber E, Fredericksen TS, Pena M (2005) Sustainability of timber harvesting in Bolivian tropical forests. *For Ecol Manage* 214:294–304.
31. Peña-Claros M, et al. (2008) Beyond reduced-impact logging: Silvicultural treatments to increase growth rates of tropical trees. *For Ecol Manage* 256:1458–1467.
32. Huth A, Ditzer T (2001) Long-term impacts of logging in a tropical rain forest—A simulation study. *For Ecol Manage* 142(1-3):33–51.
33. Bacha CJC, Rodriguez LCE (2007) Profitability and social impacts of reduced impact logging in the Tapajos National Forest, Brazil–A case study. *Ecol Econ* 63(1):70–77.
34. Keller M, Palace M, Hurtt G (2001) Biomass estimation in the Tapajos National Forest, Brazil Examination of sampling and allometric uncertainties. *For Ecol Manage* 154:371–382.
35. Rice AH, et al. (2004) Carbon balance and vegetation dynamics in an old-growth Amazonian forest. *Ecol Appl* 14(4):55–71.
36. Miller SD, Goulden ML, Menton MC, da Rocha HR, de Freitas HC (2004) Biometric and micrometeorological measurements of tropical forest carbon balance. *Ecol Appl* 14 (4):114–126.
37. Wofsy SC, Saleska SR, Pyle EH, Hutyra LR (2007) LBA-ECO CD-10 Tree DBH Measurements at the km 67 Tower Site, Tapajos National Forest. *Oak Ridge National Laboratory Distributed Active Archive Center.* Available at: http://www.daac.ornl.gov. Accessed November 5, 2011.
38. Menton M, et al. (2011) LBA-ECO CD-04 Biomass Survey, km 83 Tower Site, Tapajos National Forest. *Oak Ridge National Laboratory Distributed Active Archive Center.* Available at: http://daac.ornl.gov. Accessed November 5, 2011.
39. Liming FG (1957) Homemade dendrometers. *J For* 55:575–577.
40. Chambers JQ, Santos J, Ribeiro RJ, Higuchi N (2001) Tree damage, allometric relationships, and above-ground net primary production in central Amazon forest. *For Ecol Manage* 152(1-3):73–84.
41. Rice AH, et al. (2007) LBA-ECO CD-10 Ground-based Biometry Data at km 67 Tower Site, Tapajos National Forest. *Oak Ridge National Laboratory Distributed Active Archive Center.* Available at: http://www.daac.ornl.gov. Accessed November 5, 2011.
42. Figueira AMS, et al. (2011) LBA-ECO CD-04 Dendrometry, km 83 Tower Site, Tapajos National Forest, Brazil. *Oak Ridge National Laboratory Distributed Active Archive Center.* Available at: http://daac.ornl.gov.
43. Figueira AMS, et al. (2011) LBA-ECO CD-04 Leaf Litter Data, km 83 Tower Site, Tapajos National Forest, Brazil. *Oak Ridge National Laboratory Distributed Active Archive Center.* Available at: http://daac.ornl.gov.
44. Goulden ML, et al. (2004) Diel and seasonal patterns of tropical forest CO2 exchange. *Ecol Appl* 14(4):42–54.
45. Hutyra LR, et al. (2007) Seasonal controls on the exchange of carbon and water in an Amazonian rain forest. *J Geophys Res* 112:G03008.
46. Saleska SR, et al. (2003) Carbon in Amazon forests: Unexpected seasonal fluxes and disturbance-induced losses. *Science* 302:1554–1557.
47. Hutyra L, Wofsy SC, Saleska SR (2007) LBA-ECO CD-10 CO2 and H2O Eddy Fluxes at km 67 Tower Site, Tapajos National Forest. *Oak Ridge National Laboratory Distributed Active Archive Center.* Available at: http://www.daac.ornl.gov. Accessed November 5, 2011.
48. Miller SD, Goulden ML, Rocha HR (2009) LBA-ECO CD-04 Meteorological and Flux Data, km 83 Tower Site, Tapajos National Forest. *Oak Ridge National Laboratory Distributed Active Archive Center.* Available at: http://daac.ornl.gov.
49. Miller SD, Goulden ML, Rocha HR (2009) LBA-ECO CD-04 CO2 Profiles, km 83 Tower Site, Tapajos National Forest. *Oak Ridge National Laboratory Distributed Active Archive Center.* Available at: http://daac.ornl.gov.
50. Hutyra LR, et al. (2008) Resolving systematic errors in estimates of net ecosystem exchange of CO2 and ecosystem respiration in a tropical forest biome. *Agric For Meteorol* 148:1266–1279.
51. Goulden ML, Miller SD, da Rocha HR (2010) LBA-ECO CD-04 Soil Moisture Data, km 83 Tower Site, Tapajos National Forest, Brazil. *Oak Ridge National Laboratory Distributed Active Archive Center.* Available at: http://daac.ornl.gov. Accessed November 5, 2011.
52. Silver WL, et al. (2005) Fine root dynamics and trace gas fluxes in two lowland tropical forest soils. *Glob Change Biol* 11:290–306.
53. Palace M, Keller M, Asner GP, Silva J, Passos C (2007) Necromass in undisturbed and logged forests in the Brazilian Amazon. *For Ecol Manage* 238:309–318.
54. Telles ECC, et al. (2003) Influence of soil texture on carbon dynamics and storage potential in tropical forest soils of Amazonia. *Global Biogeochem Cycles* 17:1040.